



基于多孔介质理论的径向非均质饱和土-圆形隧道衬砌稳态响应研究

闫启方, 刘林超

引用本文:

闫启方, 刘林超. 基于多孔介质理论的径向非均质饱和土-圆形隧道衬砌稳态响应研究[J]. 信阳师范学院学报自然科学版, 2024, 37(4): 498-507. doi: 10.3969/j.issn.1003-0972.2024.04.012

YAN Qifang, LIU Linchao. Steady State Response of Radial Heterogeneous Saturated Soil-circular Tunnel Lining Based on Theory of Porous Medium[J]. Journal of Xinyang Normal University (Natural Science Edition), 2024, 37(4): 498-507. doi: 10.3969/j.issn.1003-0972.2024.04.012

在线阅读 View online: <https://doi.org/10.3969/j.issn.1003-0972.2024.04.012>

您可能感兴趣的其他文章

Articles you may be interested in

基于多孔介质理论的径向非均质饱和土中管桩的扭转振动

Torsional Vibration of a Single Pipe Pile in Radial Heterogeneous Saturated Soil Based on Theory of Porous Medium

信阳师范学院学报自然科学版, 2018, 31(2): 312-317. <https://doi.org/10.3969/j.issn.1003-0972.2018.02.027>

基于动力相互作用因子的饱和土中群管桩的纵向振动研究

Study on Longitudinal Vibration of Pipe Pile Groups in Saturated Soil Based on Dynamic Interaction Factor

信阳师范学院学报自然科学版, 2017, 30(4): 651-657. <https://doi.org/10.3969/j.issn.1003-0972.2017.04.030>

分数黏弹性可压缩油气井管杆准静态响应分析

Quasi-static Response Analysis of Fractional Viscoelastic Compressible Oil and Gas Well Pipe Rod

信阳师范学院学报自然科学版, 2021, 34(2): 331-338,344. <https://doi.org/10.3969/j.issn.1003-0972.2021.02.026>

分数阶黏弹性不可压缩油气井管杆动态力学响应

Dynamic Mechanical Response of Fractional Derivative Viscoelastic Incompressible Oil and Gas Wells Tube

信阳师范学院学报自然科学版, 2020, 33(3): 480-486. <https://doi.org/10.3969/j.issn.1003-0972.2020.03.024>

部分外露摩擦管桩的扭转振动研究

Studies on the Torsional Vibration of Partially Exposed Friction Pipe Pile

信阳师范学院学报自然科学版, 2021, 34(3): 489-494. <https://doi.org/10.3969/j.issn.1003-0972.2021.03.025>

基于多孔介质理论的径向非均质饱和土-圆形 隧道衬砌稳态响应研究

闫启方*, 刘林超

(信阳师范大学 建筑与土木工程学院, 河南 信阳 464000)

摘要:考虑土体液相、施工和地应力等对隧道周围土体的影响,将隧道周围土体看作非均质饱和土,假设固相剪切模量沿径向变化。采用多圈层模型,将隧道周围饱和土划分为未扰动区域饱和土和扰动区域饱和土,扰动区域饱和土又划分为多个薄层同心环。求解了未扰动区域饱和土和各圈层饱和土的稳态解,得到了扰动区域饱和土外边界与内边界处固相位移、液相径向位移和固相径向应力之间的传递矩阵。将圆形隧道衬砌视为弹性介质,利用弹性动力学理论,得到了圆形隧道衬砌的径向位移和径向应力。考虑问题的接触面处的连续性条件和边界条件,得到了径向非均质饱和土-圆形隧道衬砌稳态响应的解析解。数值算例表明:饱和土固相径向位移和径向应力随频率变化曲线存在较为明显的波峰和波谷,且在 $R\omega/v=1.0$ 附近存在一定的突变。影响区域剪切模量比和剪切模量沿径向的变化规律,对非均质饱和土-圆形隧道衬砌的稳态响应有较大的影响,非均质特性和液相对饱和土-圆形隧道衬砌系统动力特性的影响,不能被忽略。

关键词:非均质饱和土;圆形隧道衬砌;多孔介质理论;多圈层模型;稳态响应

中图分类号:TU435 文献标识码:A

开放科学(资源服务)标识码(OSID):



Steady State Response of Radial Heterogeneous Saturated Soil-circular Tunnel Lining Based on Theory of Porous Medium

YAN Qifang*, LIU Linchao

(College of Architecture and Civil Engineering, Xinyang Normal University, Xinyang 464000, China)

Abstract: Considering the influence of liquid phase of soil, construction and in-situ stress on the soil around the tunnel, the soil around the tunnel was regarded as heterogeneous saturated soil, and it was assumed that the solid shear modulus of solid phase changed along the radial direction. Using the multi circle model, the saturated soil around the tunnel was divided into the undisturbed saturated soil and disturbed saturated soil, and the disturbed saturated soil was divided into multiple thin concentric rings. The steady-state solutions of saturated soil in undisturbed area and each circle were solved, and the transfer matrix between radial displacement of solid phase and liquid-phase, radial stress of solid phase at the outer and inner boundaries of saturated soil in the disturbed region was obtained. Taking the circular tunnel lining as elastic medium, the radial displacement and radial stress of the circular tunnel lining were obtained by using the elastic dynamics theory. Considering the continuity condition and the boundary condition of the problem, the analytical solution of the steady-state response of radial heterogeneous saturated soil-circular tunnel lining was obtained. Numerical examples showed that there were obvious peaks and troughs in the curves of radial displacement and radial stress of saturated soil varying with frequency, and there was a certain mutation near when $R\omega/v=1.0$. The ratio of shear modulus in the affected area and the variation law of shear modulus along the radial direction had a great influence on the

收稿日期:2023-08-31;修回日期:2023-11-23;*.通信联系人,E-mail:yqf815@126.com

基金项目:国家自然科学基金项目(U1504505);河南省高等学校重点科研项目(23B560001)

作者简介:闫启方(1979—),女,河南驻马店人,副教授,硕士,硕士生导师,主要从事结构动力学的研究。

引用格式:闫启方,刘林超.基于多孔介质理论的径向非均质饱和土-圆形隧道衬砌稳态响应研究[J].信阳师范学院学报(自然科学版),2024,37(4):498-507.

YAN Qifang, LIU Linchao. Steady State Response of Radial Heterogeneous Saturated Soil-circular Tunnel Lining Based on Theory of Porous Medium[J]. Journal of Xinyang Normal University (Natural Science Edition), 2024, 37(4): 498-507.

steady-state response of heterogeneous saturated soil-circular tunnel lining system, and the influence of tunnel lining thickness had a certain relationship with frequency. The influence of heterogeneous characteristics and the liquid phase on the dynamic characteristics of saturated soil-circular tunnel lining system could not be ignored.

Key words: heterogeneous saturated soil; circular tunnel lining; theory of porous medium; multi-cycle model; steady state response

0 引言

近年来,铁路、地铁、综合管廊等工程建设发展迅速,对地下工程结构特别是隧道工程动力特性的研究可以为地下工程结构安全稳定提供重要的理论基础,同时对隧道工程结构的抗震设计、动力监测等都具有十分重要的意义。因此,近年来不少学者对隧道结构动态激励下的动力响应和动态特性进行了研究^[1-3]。

土体力学性质对地下工程结构动力稳定的影响很大,因此需要开展复杂地质中隧道工程结构动力特性的研究。影响土体力学性质的因素主要有自然力学特性和外部因素两个方面。自然力学特性如饱和土、黏弹性特性等,当土体气相完全被液体充满时即为饱和土,饱和土存在广泛。针对饱和土中隧道的动态力学响应问题,XIE等^[4]在Biot波动方程的基础上对黏弹性饱和土中部分封闭衬砌圆形隧道的动力响应进行了研究,在拉普拉斯变换域内得到了轴对称逐步加载引起的应力、位移和孔隙压力的解析解。WANG等^[5]将衬砌结构和周围土体分别被视为均质弹性介质和饱和多孔介质,对衬砌隧道在爆破作用下的三维动力响应进行了研究,通过傅立叶变换和拉普拉斯变换,推导了饱和土中位移、应力和孔隙水压力以及地表位移的时域三维解。基于Biot饱和土理论,HU等^[6]研究了移动荷载作用下,半空间饱和土中圆形隧道的动力响应问题。需要指出的是,这些研究都是基于Biot饱和土理论开展的,尽管Biot理论已成功应用于诸多工程领域中,但其理论模型存在一定的缺陷^[7]。而基于连续介质混合物公理和体积分数概念的多孔介质理论,能够将若干的微观性质直接通过宏观性质来描述,在不需要额外的假定下,可以将动力、材料和几何非线性等很容易地反映在数学模型中。基于多孔介质理论,高华喜等^[8]将衬砌视为具有分数导数本构关系的多孔黏弹性体,利用饱和多孔介质理论,研究了内水压力作用下饱和黏弹性土和衬砌系统的振动特性。杨骁等^[9]在饱和多

孔介质理论和平面弹性理论的基础上,对分数导数型黏弹性饱和土体和深埋圆形隧洞弹性衬砌相互作用的耦合简谐振动进行了研究,给出了饱和黏弹性土、弹性衬砌简谐振动的频域解析解。

影响土体力学性质外部因素如施工、地应力等。对于隧道周围的土体,施工和地应力等的干扰作用通常会导致隧道周围土体力学性质的变化,如剪切模量沿径向的变化,从而导致隧道周围土体的非均匀性。然而,目前针对非均质土-隧道结构的研究,还未见报道。随着隧道等地下工程结构的快速发展,对于复杂地质条件下隧道动力特性的研究就显得格外重要,因此有必要开展非均质饱和土-圆形隧道衬砌结构的动力相互作用的研究,将为非均质土体中隧道的设计和施工提供帮助。因此,本文在考虑隧道周围土体的非均质性和土体液相影响的情况下,通过数学物理手段研究径向非均质饱和土-圆形隧道衬砌的稳态响应问题。

1 径向非均质饱和土-圆形隧道衬砌模型

考察无限饱和土中深埋圆形隧道衬砌结构,如图1所示。

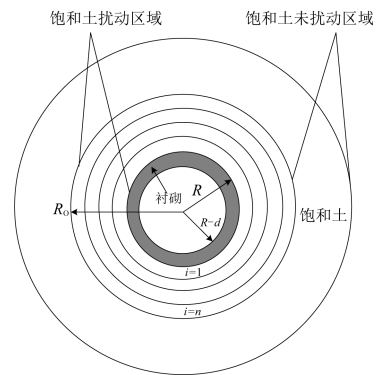


图1 径向非均质饱和土-圆形隧道衬砌模型

Fig. 1 Model of radially inhomogeneous saturated soil-circular tunnel lining

圆形隧道洞内衬为混凝土弹性衬砌,作用有幅值为 q_0 的简谐内压力 $q = q_0 e^{i\omega t}$,简谐内压力的频率为 ω , i 代表虚数单位。圆形隧道衬砌的半径和厚度分别为 R 和 d ,将圆形衬砌周围的土体视为两相饱和土,在沿径向 R 到 R_0 范围内饱和土发生

了扰动,导致饱和土固相剪切模量沿半径发生了如图2所示的变化,参考文献[10-11],设饱和土固相剪切模量符合如下公式:

$$\mu(r) = \begin{cases} \mu_0^s f(r), & R < r < R_0, \\ \mu_0^s, & r \geq R_0, \end{cases} \quad (1)$$

$$f(r) = 1 - \left(1 - \frac{\mu_1^s}{\mu_0^s}\right) \left(\frac{R_0 - r}{R_s}\right)^m, \quad (2)$$

式中: μ_0^s 和 μ_1^s 分别为未扰动区域和隧道衬砌与土体交界处饱和土固相剪切模量, R_s 为饱和土沿径向的扰动长度, m 为正的幂指数。定义影响区域土体模量比 $\mu = \mu_1^s / \mu_0^s$ 。

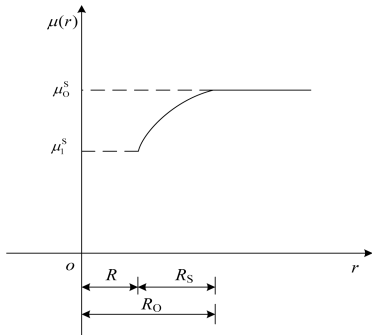


图2 饱和土固相剪切模量沿径向变化规律

Fig. 2 The change rules of shear modulus of solid phase of saturated soil with the radial direction

2 径向非均质饱和土-圆形隧道衬砌简谐振动的多圈层模型解

根据圆形隧道周围土体的性质,将饱和土划分为未扰动和扰动区域,见图1。同时,将扰动区域的饱和土再划分为 n 个薄层同心环区域,这样就可以将每个薄层同心环区域饱和土视为均质饱和土。对于圆形隧道衬砌周围饱和土体采用多孔介质理论来描述,在极坐标下,仅考虑径向和环向位移,由参考文献[12-13]可得未扰动区域饱和土和扰动区域第 i 层饱和土的控制方程为:

未扰动区域饱和土

$$\frac{2-2\nu_0}{1-2\nu_0} \mu_0^s \frac{\partial}{\partial r} \left(\frac{\partial u_{Or}^s}{\partial r} + \frac{u_{Or}^s}{r} \right) - n_0^s \frac{\partial p}{\partial r} - \rho_0^s \frac{\partial^2 u_{Or}^s}{\partial t^2} + S_{Ov} \left(\frac{\partial u_{Or}^F}{\partial t} - \frac{\partial u_{Or}^s}{\partial t} \right) = 0, \quad (3)$$

$$n_0^F \frac{\partial p}{\partial r} + \rho_0^F \frac{\partial^2 u_{Or}^F}{\partial t^2} + S_{Ov} \left(\frac{\partial u_{Or}^F}{\partial t} - \frac{\partial u_{Or}^s}{\partial t} \right) = 0, \quad (4)$$

$$\frac{1}{r} \frac{\partial}{\partial r} \left[r \left(n_0^s \frac{\partial u_{Or}^s}{\partial t} + n_0^F \frac{\partial u_{Or}^F}{\partial t} \right) \right] = 0. \quad (5)$$

扰动区域第 i 圈层饱和土

$$\frac{2-2\nu_{0i}}{1-2\nu_{0i}} \mu_{0i}^s \frac{\partial}{\partial r} \left(\frac{\partial u_{Oir}^s}{\partial r} + \frac{u_{Oir}^s}{r} \right) - n_i^s \frac{\partial p_i}{\partial r} -$$

$$\rho_{0i}^s \frac{\partial^2 u_{Oir}^s}{\partial t^2} + S_{Oiv} \left(\frac{\partial u_{Oir}^F}{\partial t} - \frac{\partial u_{Oir}^s}{\partial t} \right) = 0, \quad (6)$$

$$n_i^F \frac{\partial p_i}{\partial r} + \rho_{0i}^F \frac{\partial^2 u_{Oir}^F}{\partial t^2} + S_{Oiv} \left(\frac{\partial u_{Oir}^F}{\partial t} - \frac{\partial u_{Oir}^s}{\partial t} \right) = 0, \quad (7)$$

$$\frac{1}{r} \frac{\partial}{\partial r} \left[r \left(n_i^s u_{Oir}^s + n_i^F u_{Oir}^F \right) \right] = 0, \quad (8)$$

式中: u_{Or}^s 和 u_{Or}^F 、 u_{Oir}^s 和 u_{Oir}^F 分别为未扰动区域、扰动区域第 i 圈层饱和土固相和液相的径向位移; n_0^s 和 n_0^F 、 n_i^s 和 n_i^F 分别为未扰动区域、扰动区域第 i 圈层饱和土固相和液相的体积分数,且满足 $n_0^s + n_0^F = 1$, $n_i^s + n_i^F = 1$; μ_0^s 、 μ_{0i}^s 分别为未扰动区域、扰动区域第 i 层饱和土固相的剪切模量; ν_0 、 ν_{0i} 分别为未扰动区域、扰动区域第 i 圈层饱和土固相泊松比; ρ_0^s 和 ρ_{0i}^s 、 ρ_{0i}^F 和 ρ_{0i}^F 分别为扰动区域、扰动区域第 i 圈层饱和土固相和液相表观密度; p 、 p_i 分别为未扰动区域、扰动区域第 i 圈层饱和土孔隙水压力; S_{Ov} 、 S_{Oiv} 分别为未扰动区域、扰动区域第 i 圈层饱和土液固耦合系数。

由于圆形隧道在简谐内压力作用下将做稳态振动,未扰动区域和扰动区域第 i 圈层饱和土固相土径向位移、液相径向位移和固相径向应力满足

$$u_{Or}^s = \tilde{u}_{Or}^s e^{i\omega t}, u_{Or}^F = \tilde{u}_{Or}^F e^{i\omega t}, u_{Oir}^s = \tilde{u}_{Oir}^s e^{i\omega t}, \\ u_{Oir}^F = \tilde{u}_{Oir}^F e^{i\omega t}, \sigma_{Orr}^{SE} = \tilde{\sigma}_{Orr}^{SE} e^{i\omega t}, \sigma_{irr}^{SE} = \tilde{\sigma}_{irr}^{SE} e^{i\omega t},$$

式中: \tilde{u}_{Or}^s 、 \tilde{u}_{Or}^F 、 \tilde{u}_{Oir}^s 、 \tilde{u}_{Oir}^F 、 $\tilde{\sigma}_{Orr}^{SE}$ 、 $\tilde{\sigma}_{irr}^{SE}$ 分别为未扰动区域和扰动区域第 i 圈层饱和土固相径向位移、液相径向位移和径向应力的幅值,将其代入式(3)一式(8),并令

$$U_0^s = \frac{\tilde{u}_{Or}^s}{R}, U_0^F = \frac{\tilde{u}_{Or}^F}{R}, U_i^s = \frac{\tilde{u}_{Oir}^s}{R}, U_i^F = \frac{\tilde{u}_{Oir}^F}{R},$$

$$\bar{r} = \frac{r}{R}, \bar{\omega} = \frac{R\omega}{v_0}, v_0 = \sqrt{\frac{\mu_0^s}{\rho_0^s}}, s_0 = \frac{RS_{Ov}}{\rho_0^s v_0},$$

$$\delta = \frac{d}{R}, \eta_0 = 1 - \delta, \delta = \frac{d}{R}, P = \frac{p}{\mu_0^s}, P_i = \frac{p_i}{\mu_0^s},$$

$$\mu_i = \frac{\mu_{0i}^s}{\mu_0^s}, \eta_0 = \frac{R-d}{R} = 1 - \delta, \rho_0 = \frac{\rho_0^F}{\rho_0^s},$$

$$s_i = \frac{S_{Oiv}}{S_{Ov}}, \rho_i = \frac{\rho_{0i}^s}{\rho_0^s}, \rho_{0i} = \frac{\rho_{0i}^F}{\rho_{0i}^s},$$

可得

$$\frac{2-2\nu_0}{1-2\nu_0} \frac{\partial}{\partial \bar{r}} \left(\frac{\partial U_0^s}{\partial \bar{r}} + \frac{U_0^s}{\bar{r}} \right) - n_0^s \frac{\partial P}{\partial \bar{r}} + \bar{\omega}^2 U_0^s + i\bar{\omega} s_0 (U_0^F - U_0^s) = 0, \quad (9)$$

$$n_0^F \frac{\partial P}{\partial \bar{r}} - \rho_0 \bar{\omega}^2 U_0^F + i\bar{\omega} s_0 (U_0^F - U_0^s) = 0, \quad (10)$$

$$\frac{1}{r} \frac{\partial}{\partial r} [r(n_0^S U_0^S + n_0^F U_0^F)] = 0, \quad (11)$$

$$\frac{2-2\nu_{0i}}{1-2\nu_{0i}} \mu_i \frac{\partial}{\partial r} \left(\frac{\partial U_i^S}{\partial r} + \frac{U_i^S}{r} \right) - n_{0i}^S \mu_i \frac{\partial P_i}{\partial r} + \rho_i \bar{\omega}^2 U_{0i}^S + i \bar{\omega} s_i s_0 (U_i^F - U_i^S) = 0, \quad (12)$$

$$n_{0i}^F \frac{\partial P_i}{\partial r} - \rho_i \rho_{0i} \bar{\omega}^2 U_{0i}^F + i s_i s_0 \bar{\omega} (U_i^F - U_i^S) = 0, \quad (13)$$

$$\frac{1}{r} \frac{\partial}{\partial r} [r(n_i^S U_i^S + n_i^F U_i^F)] = 0. \quad (14)$$

为了求解方程式(9)–(14), 引入势函数:

$$\begin{cases} U_0^S = \frac{\partial \Phi_0}{\partial r}, U_0^F = \frac{\partial \Psi_0}{\partial r}, \\ U_i^S = \frac{\partial \Phi_i}{\partial r}, U_i^F = \frac{\partial \Psi_i}{\partial r}. \end{cases} \quad (15)$$

将式(15)代入方程式(9)–(14), 解耦可得

$$\begin{cases} \frac{2-2\nu_0}{1-2\nu_0} \Delta \Phi_0 - n_0^S P + \bar{\omega}^2 \Phi_0 + i \bar{\omega} s_0 (\Psi_0 - \Phi_0) = 0, \\ n_0^F P - \rho_0 \bar{\omega}^2 \Psi_0 + i \bar{\omega} s_0 (\Psi_0 - \Phi_0) = 0, \\ n_0^S \Delta \Phi_0 + n_0^F \Delta \Psi_0 = 0, \end{cases} \quad (16)$$

$$\begin{cases} \frac{2-2\nu_{0i}}{1-2\nu_{0i}} \Delta \Phi_i - n_i^S \frac{\partial P_i}{\partial r} + \frac{\rho_i \bar{\omega}^2}{\mu_i} \Phi_i + \frac{i \bar{\omega} s_i s_0}{\mu_i} (\Psi_i - \Phi_i) = 0, \\ n_i^F P - \rho_i \rho_{0i} \bar{\omega}^2 \Psi_i + i s_i s_0 \bar{\omega} (\Psi_i - \Phi_i) n_i^S \Delta \Phi_i + n_i^F \Delta \Psi_i = 0, \end{cases} \quad (17)$$

式中: $\Delta = \frac{\partial^2}{\partial r^2} + \frac{1}{r} \frac{\partial}{\partial r}$ 为拉普拉斯算子。

由式(16)和式(17)可得

$$\Delta(\Delta - h_0^2) \Phi_0 = 0, \quad (18)$$

$$\Delta(\Delta - h_i^2) \Phi_i = 0, \quad (19)$$

式中:

$$h_0^2 = \frac{n_0^S \beta_{02}}{n_0^F} - \beta_{01}, h_i^2 = \beta_{i2} \frac{n_i^S}{n_i^F} - \beta_{i1},$$

$$\beta_{01} = \frac{1-2\nu_0 n_0^F \bar{\omega}^2 - i \bar{\omega} s_0}{2-2\nu_0 n_0^F},$$

$$\beta_{02} = \frac{1-2\nu_0 i \bar{\omega} s_0 - n_0^S \rho_0 \bar{\omega}^2}{2-2\nu_0 n_0^F},$$

$$\beta_{i1} = \frac{1-2\nu_{0i} n_i^F \rho_i \bar{\omega}^2 - i n_i^S s_i s_0 \mu_i \bar{\omega} - i \bar{\omega} s_i s_0 n_i^F}{2-2\nu_{0i} n_i^F \mu_i},$$

$$\beta_{i2} = \frac{1-2\nu_{0i} i n_i^F \bar{\omega} s_i s_0 - n_i^S \mu_i \rho_{0i} \bar{\omega}^2 + i n_i^S \mu_i s_i s_0 \bar{\omega}}{2-2\nu_{0i} n_i^F \mu_i}.$$

根据算子分解理论, 令

$$\Phi_0 = \varphi_{01} + \varphi_{02}, \quad (20)$$

代入式(18)可得

$$(\Delta - h_0^2) \varphi_{01} = 0, \quad (21)$$

$$\Delta \varphi_{02} = 0. \quad (22)$$

求解式(21)和式(22), 考虑无穷远处位移为零, 得

$$\begin{aligned} \Phi_0 &= A_{01} K_0(h_0 \bar{r}) + B_{01} I_0(h_0 \bar{r}) + D_{01} \ln \bar{r}. \end{aligned} \quad (23)$$

同理, 可得

$$\begin{aligned} \Phi_i &= A_{i1} K_0(h_i \bar{r}) + B_{i1} I_0(h_i \bar{r}) + C_{i1} + D_{i1} \ln \bar{r}, \end{aligned} \quad (24)$$

式中的待定系数 A_{01} 、 A_{02} 、 A_{i1} 、 B_{i1} 、 D_{i1} 可以根据边界条件和连续性条件确定。

由式(15)可得未扰动区域饱和土和扰动区域第 i 层饱和土固相和液相的径向位移分别为:

$$U_0^S = -A_{01} h_0 K_1(h_0 \bar{r}) + \frac{1}{r} D_{01}, \quad (25)$$

$$U_0^F = \frac{h_0^2 + \beta_{01}}{\beta_{02}} h_0 K_1(h_0 \bar{r}) A_{01} - \frac{\beta_{01}}{\beta_{02} r} D_{01}, \quad (26)$$

$$\begin{aligned} U_i^S &= -A_{i1} h_i K_1(h_i \bar{r}) + B_{i1} h_i I_1(h_i \bar{r}) + \frac{1}{r} D_{i1}, \end{aligned} \quad (27)$$

$$\begin{aligned} U_i^F &= \frac{h_i^2 + \beta_{i1}}{\beta_{i2}} h_i K_1(h_i \bar{r}) A_{i1} - \frac{h_i^2 + \beta_{i1}}{\beta_{i2}} h_i I_1(h_i \bar{r}) B_{i1} - \frac{\beta_{i1}}{\beta_{i2} r} D_{i1}. \end{aligned} \quad (28)$$

由应力和位移关系, 可以得到未扰动区域饱和土和扰动区域第 i 圈层饱和土固相径向应力分别为:

$$\begin{aligned} \bar{\sigma}_{Orr}^{SE} &= \left[\frac{2-2\nu_0}{1-2\nu_0} h_0^2 K_0(h_0 \bar{r}) + h_0 \frac{2}{r} K_1(h_0 \bar{r}) \right] A_{01} + \left[\frac{2-2\nu_0}{1-2\nu_0} h_0^2 I_0(h_0 \bar{r}) - h_0 \frac{2}{r} I_1(h_0 \bar{r}) \right] B_{01} - \frac{2}{r^2} D_{01}, \end{aligned} \quad (29)$$

$$\begin{aligned} \bar{\sigma}_{irr}^{SE} &= \left[\frac{2-2\nu_{0i}}{1-2\nu_{0i}} h_i^2 K_0(h_i \bar{r}) + h_i \frac{2}{r} K_1(h_i \bar{r}) \right] \mu_i A_{i1} + \left[\frac{2-2\nu_{0i}}{1-2\nu_{0i}} h_i^2 I_0(h_i \bar{r}) - \right. \end{aligned}$$

$$h_i \frac{2}{r} I_1(h_i \bar{r}) \mu_i B_{i1} - \frac{2}{r^2} \mu_i D_{i1} \quad (30)$$

对于扰动区域第 i 圈层饱和土, 在第 i 圈层饱和土与第 $i-1$ 圈层饱和土交界处(即 $\bar{r} = \bar{r}_i$) 的固相径向位移与径向应力分别为

$$U_i^S(\bar{r}_{i-1}) = -A_{i1} h_i K_1(h_i \bar{r}_{i-1}) + B_{i1} h_i I_1(h_i \bar{r}_{i-1}) + \frac{1}{r_{i-1}} D_{i1}, \quad (31)$$

$$U_i^F(\bar{r}_{i-1}) = \frac{h_i^2 + \beta_{i1}}{\beta_{i2}} h_i K_1(h_i \bar{r}_{i-1}) A_{i1} - \frac{h_i^2 + \beta_{i1}}{\beta_{i2}} h_i I_1(h_i \bar{r}_{i-1}) B_{i1} - \frac{\beta_{i1}}{\beta_{i2} r_{i-1}} D_{i1}, \quad (32)$$

$$\begin{aligned} \bar{\sigma}_{irr}^{SE}(\bar{r}_{i-1}) = & \left[\frac{2-2\nu_{Oi}}{1-2\nu_{Oi}} h_i^2 K_0(h_i \bar{r}_{i-1}) + \right. \\ & h_i \frac{2}{r_{i-1}} K_1(h_i \bar{r}_{i-1}) \left. \right] \mu_i A_{i1} + \\ & \left[\frac{2-2\nu_{Ox}}{1-2\nu_{Ox}} h_i^2 I_0(h_i \bar{r}_{i-1}) - h_i \frac{2}{r_{i-1}} I_1(h_i \bar{r}_{i-1}) \right] \cdot \\ & \mu_i B_{i1} - \frac{2}{r_{i-1}^2} \mu_i D_{i1}. \quad (33) \end{aligned}$$

由初始参数法得第 i 圈层外边界处和内边界处固相径向位移、液相径向位移和固相径向应力的关系为

$$\begin{aligned} U_i^S(\bar{r}_i) = & -\frac{1-2\nu_{Oi} N_i U_i^S(\bar{r}_{i-1})}{1-\nu_{Oi} h_i \bar{r}_{i-1} M_i} - \\ & \frac{\beta_{i1} F_i U_i^S(\bar{r}_{i-1}) + (\frac{\bar{r}_{i-1}}{r_i} + \frac{\beta_{i1} \bar{r}_{i-1}}{h_i^2 \bar{r}_i}) U_i^S(\bar{r}_{i-1}) +}{h_i^2 M_i} \\ & \frac{\beta_{i2} \bar{r}_{i-1} U_i^F(\bar{r}_{i-1}) - \beta_{i2} F_i U_i^F(\bar{r}_{i-1}) -}{\bar{r}_i h_i^2} \\ & \frac{1-2\nu_{Oi} N_i \bar{\sigma}_{irr}^{SE}(\bar{r}_{i-1})}{2-2\nu_{Oi} \mu_i h_i M_i}, \quad (34) \end{aligned}$$

$$\begin{aligned} U_i^F(\bar{r}_i) = & \frac{h_i^2 + \beta_{i1} \beta_{i1} F_i}{\beta_{i2} h_i^2 M_i} U_i^S(\bar{r}_{i-1}) + \\ & \frac{h_i^2 + \beta_{i1} 1 - 2\nu_{Oi}}{\beta_{i2} 2 - 2\nu_{Oi} h_i \bar{r}_{i-1} M_i} \frac{2N_i}{2 - 2\nu_{Oi} h_i \bar{r}_{i-1} M_i} U_i^S(\bar{r}_{i-1}) - \\ & \frac{\beta_{i1}}{\beta_{i2}} \left(\frac{\bar{r}_{i-1}}{r_i} + \frac{\beta_{i1} \bar{r}_{i-1}}{\bar{r}_i h_i^2} \right) U_i^S(\bar{r}_{i-1}) + \\ & \frac{h_i^2 + \beta_{i1} \beta_{i2} F_i}{\beta_{i2} h_i^2 M_i} U_i^F(\bar{r}_{i-1}) - \\ & \frac{\beta_{i1} \bar{r}_{i-1} U_i^F(\bar{r}_{i-1})}{h_i^2 \bar{r}_i} \frac{h_i^2 + \beta_{i1} 1 - 2\nu_{Oi}}{\beta_{i2} 2 - 2\nu_{Oi}} \cdot \\ & \frac{N_i}{\mu_i h_i M_i} \bar{\sigma}_{irr}^{SE}(\bar{r}_{i-1}), \quad (35) \end{aligned}$$

$$\begin{aligned} \bar{\sigma}_{irr}^{SE}(\bar{r}_i) = & \frac{L_i}{M_i} \bar{\sigma}_{irr}^{SE}(\bar{r}_{i-1}) + \\ & \frac{1-2\nu_{Oi} N_i}{1-\nu_{Oi} h_i \bar{r}_i M_i} \bar{\sigma}_{irr}^{SE}(\bar{r}_{i-1}) + \\ & \frac{2-2\nu_{Oi} \mu_i \beta_{i1} G_i}{1-2\nu_{Oi} h_i M_i} U_i^S(\bar{r}_{i-1}) + \\ & \frac{2\mu_i \beta_{i1} F_i}{h_i^2 \bar{r}_i M_i} U_i^S(\bar{r}_{i-1}) + \frac{2\mu_i L_i}{r_{i-1} M_i} U_i^S(\bar{r}_{i-1}) + \\ & \frac{1-2\nu_{Oi}}{1-\nu_{Oi} h_i \bar{r}_i \bar{r}_{i-1} M_i} U_i^S(\bar{r}_{i-1}) - \\ & 2\mu_i \left(\frac{\bar{r}_{i-1}}{r_i^2} + \frac{\beta_{i1} \bar{r}_{i-1}}{r_i^2 h_i^2} \right) U_i^S(\bar{r}_{i-1}) + \\ & \frac{2-2\nu_{Oi} \mu_i \beta_{i2} G_i}{1-2\nu_{Oi} h_i M_i} U_i^F(\bar{r}_{i-1}) + \\ & \frac{2\mu_i \beta_{i2} F_i}{h_i^2 \bar{r}_i M_i} U_i^F(\bar{r}_{i-1}) - \frac{2\mu_i \beta_{i2} \bar{r}_{i-1}}{\bar{r}_i^2 h_i^2} U_i^F(\bar{r}_{i-1}), \quad (36) \end{aligned}$$

式中:

$$\begin{aligned} M_i = & K_0(h_i \bar{r}_{i-1}) I_1(h_i \bar{r}_{i-1}) + \\ & K_1(h_i \bar{r}_{i-1}) I_0(h_i \bar{r}_{i-1}), \\ N_i = & K_1(h_i \bar{r}_i) I_1(h_i \bar{r}_{i-1}) - \\ & K_1(h_i \bar{r}_{i-1}) I_1(h_i \bar{r}_i), \\ F_i = & K_1(h_i \bar{r}_i) I_0(h_i \bar{r}_{i-1}) + \\ & K_0(h_i \bar{r}_{i-1}) I_1(h_i \bar{r}_i), \\ G_i = & K_0(h_i \bar{r}_i) I_0(h_i \bar{r}_{i-1}) - \\ & K_0(h_i \bar{r}_{i-1}) I_0(h_i \bar{r}_i), \\ L_i = & K_0(h_i \bar{r}_i) I_1(h_i \bar{r}_{i-1}) + \\ & K_1(h_i \bar{r}_{i-1}) I_0(h_i \bar{r}_i), \end{aligned}$$

这里 $K_0(\cdot)$ 和 $K_1(\cdot)$ 分别为 0 阶和 1 阶第二类变形贝塞尔函数, $I_0(\cdot)$ 和 $I_1(\cdot)$ 分别为 0 阶和 1 阶第一类变形贝塞尔函数。

将式(34)一式(36)写成矩阵形式, 则有

$$\begin{bmatrix} U_i^S(\bar{r}_i) \\ U_i^F(\bar{r}_i) \\ \bar{\sigma}_{irr}^{SE}(\bar{r}_i) \end{bmatrix} = \begin{bmatrix} a_{i11} & a_{i12} & a_{i13} \\ a_{i21} & a_{i22} & a_{i23} \\ a_{i31} & a_{i32} & a_{i33} \end{bmatrix} \begin{bmatrix} U_i^S(\bar{r}_{i-1}) \\ U_i^F(\bar{r}_{i-1}) \\ \bar{\sigma}_{irr}^{SE}(\bar{r}_{i-1}) \end{bmatrix}, \quad (37)$$

式中:

$$\begin{aligned} a_{i11} = & -\frac{1-2\nu_{Oi} N_i}{1-\nu_{Oi} h_i \bar{r}_{i-1} M_i} - \frac{\beta_{i1} F_i}{h_i^2 M_i} + \\ & \frac{h_i^2 \bar{r}_{i-1} + \beta_{i1} \bar{r}_{i-1}}{h_i^2 \bar{r}_i}, \\ a_{i12} = & -\frac{\beta_{i2} F_i}{h_i^2 M_i} + \frac{\beta_{i2} \bar{r}_{i-1}}{\bar{r}_i h_i^2}, \end{aligned}$$

$$\begin{aligned}
 a_{i13} &= \frac{1-2\nu_{O_i}}{2-2\nu_{O_i}} \frac{N_i}{\mu_i h_i M_i}, \\
 a_{i21} &= \frac{\beta_{i1}(h_i^2 + \beta_{i1})F_i}{\beta_{i2} h_i^2 M_i} + \frac{(1-2\nu_{O_i})(h_i^2 + \beta_{i1})N_i}{\beta_{i2} h_i \bar{r}_{i-1} (1-\nu_{O_i}) M_i} - \\
 &\quad \frac{\beta_{i1} \bar{r}_{i-1} (h_i^2 + \beta_{i1})}{\beta_{i2} \bar{r}_i h_i^2}, \\
 a_{i22} &= \frac{(h_i^2 + \beta_{i1})F_i}{h_i^2 M_i} - \frac{\beta_{i1} \bar{r}_{i-1}}{h_i^2 \bar{r}_i}, \\
 a_{i23} &= \frac{(1-2\nu_{O_i})(h_i^2 + \beta_{i1})N_i}{(2-2\nu_{O_i})\beta_{i2} \mu_i h_i M_i}, \\
 a_{i31} &= \frac{(2-2\nu_{O_i})\mu_i \beta_{i1} G_i}{(1-2\nu_{O_i})h_i M_i} + \frac{2\mu_i \beta_{i1} F_i}{h_i^2 \bar{r}_i M_i} + \\
 &\quad \frac{2\mu_i L_i}{\bar{r}_{i-1} M_i} + \frac{2(1-2\nu_{O_i})\mu_i N_i}{(1-\nu_{O_i})h_i \bar{r}_i \bar{r}_{i-1} M_i} - \\
 &\quad \frac{2\mu_i \bar{r}_{i-1} (h_i^2 + \beta_{i1})}{\bar{r}_i^2 h_i^2}, \\
 a_{i32} &= \frac{(2-2\nu_{O_i})\mu_i \beta_{i2} G_i}{(1-2\nu_{O_i})h_i M_i} + \\
 &\quad \frac{2\mu_i \beta_{i2} F_i}{h_i^2 \bar{r}_i M_i} - \frac{2\mu_i \beta_{i2} \bar{r}_{i-1}}{\bar{r}_i^2 h_i^2}, \\
 a_{i33} &= \frac{L_i}{M_i} + \frac{(1-2\nu_{O_i})N_i}{(1-\nu_{O_i})h_i \bar{r}_i M_i}.
 \end{aligned}$$

考虑扰动区域饱和土第 $i-1$ 圈层外边界与第 i 圈层内边界处饱和土固相径向位移、液相径向位移和固相径向应力相等的连续性条件:

$$\begin{cases}
 U_i^S(\bar{r}_{i-1}) = U_{i-1}^S(\bar{r}_i), \\
 U_i^F(\bar{r}_{i-1}) = U_{i-1}^F(\bar{r}_i), \\
 \bar{\sigma}_{irr}^S(\bar{r}_{i-1}) = \bar{\sigma}_{(i-1)rr}^S(\bar{r}_i),
 \end{cases} \quad (38)$$

将连续性条件式(38)进行传递, 可得第 n 圈层饱和土外边界与第 1 圈层饱和土内边界处固相径向位移、液相径向位移和固相径向应力的传递矩阵为

$$\begin{bmatrix} U_n^S(\bar{r}_n) \\ U_n^F(\bar{r}_n) \\ \bar{\sigma}_{nr}^{SE}(\bar{r}_n) \end{bmatrix} = \begin{bmatrix} a_{11} & a_{12} & a_{13} \\ a_{21} & a_{22} & a_{23} \\ a_{31} & a_{32} & a_{33} \end{bmatrix} \begin{bmatrix} U_1^S(\bar{r}_0) \\ U_1^F(\bar{r}_0) \\ \bar{\sigma}_{1rr}^{SE}(\bar{r}_0) \end{bmatrix}, \quad (39)$$

式中:

$$\begin{bmatrix} a_{11} & a_{12} & a_{13} \\ a_{21} & a_{22} & a_{23} \\ a_{31} & a_{32} & a_{33} \end{bmatrix} = \begin{bmatrix} a_{n11} & a_{n12} & a_{n13} \\ a_{n21} & a_{n22} & a_{n23} \\ a_{n31} & a_{n32} & a_{n33} \end{bmatrix} \cdots \cdots \\
 \begin{bmatrix} a_{i11} & a_{i12} & a_{i13} \\ a_{i21} & a_{i22} & a_{i23} \\ a_{i31} & a_{i32} & a_{i33} \end{bmatrix} \cdots \cdots \begin{bmatrix} a_{111} & a_{112} & a_{113} \\ a_{121} & a_{122} & a_{123} \\ a_{131} & a_{132} & a_{133} \end{bmatrix},$$

为第 n 圈层饱和土外边界与第 1 圈层内饱和土边界处饱和土固相径向位移、液相径向位移和固相径向应力传递矩阵。

3 非均质饱和土-圆形隧道衬砌稳态响应求解

考虑混凝土圆形隧道衬砌, 将其视为弹性介质, 仅考虑衬砌的径向位移。同样地, 由于非均质饱和土-圆形隧道衬砌系统在简谐内压力作用下做稳态振动, 所以衬砌的径向位移同样满足 $u_{Cr} = \tilde{u}_{Cr} e^{i\omega t}$, 式中 u_{Cr} 为衬砌的径向位移, \tilde{u}_{Cr} 为衬砌的径向位移幅值。在极坐标下可以得到无量纲化的衬砌振动方程为

$$\frac{\partial^2 U_C}{\partial \bar{r}^2} + \frac{1}{\bar{r}} \frac{\partial U_C}{\partial \bar{r}} - \frac{U_C}{\bar{r}^2} - q_C^2 U_C = 0, \quad (40)$$

式中:

$$q_C^2 = -\frac{1-2\nu_C \bar{\rho}_C \bar{\omega}^2}{2-2\nu_C \mu_C}, \mu_C = \frac{\mu_C}{\mu_0^S}, \bar{\rho}_C = \frac{\rho_C}{\rho_0^S},$$

ν_C 、 μ_C 和 ρ_C 分别衬砌的泊松比、剪切模量和密度。贝塞尔方程式(40)的通解为

$$U_C(\bar{r}) = A_{C1} K_1(q_C \bar{r}) + A_{C2} I_1(q_C \bar{r}), \quad (41)$$

式中: A_{C1} 、 A_{C2} 为待定系数。考虑衬砌的应力和应变关系, 由式(41)可以求得衬砌的径向应力的表达式为

$$\begin{aligned}
 \bar{\sigma}_{Crr} &= -\left[\frac{2}{\bar{r}} K_1(q_C \bar{r}) + \frac{2-2\nu_C}{1-2\nu_C} q_C K_0(q_C \bar{r}) \right] \cdot \\
 &\quad \mu_C A_{C1} + \\
 &\quad \left[\frac{2-2\nu_C}{1-2\nu_C} q_C I_0(q_C \bar{r}) - \frac{2}{\bar{r}} I_1(q_C \bar{r}) \right] \mu_C A_{C2},
 \end{aligned} \quad (42)$$

在衬砌内边界处, 衬砌径向应力满足

$$\bar{\sigma}_{Crr} = Q \Big|_{\bar{r}=\eta_0}, \quad (43)$$

式中: $Q = \frac{q_0}{\mu_0^S}$, $\eta_0 = 1 - \delta$ 。衬砌外边界与扰动区域土体接触面处饱和土固相径向位移、液相径向位移和固相径向应力满足

$$\begin{cases}
 U_C(1) = U_1^S(\bar{r}_0) = U_1^F(\bar{r}_0), \\
 \bar{\sigma}_{Crr}(1) = \bar{\sigma}_{1rr}(\bar{r}_0).
 \end{cases} \quad (44)$$

扰动区域与未扰动区域饱和土交界处固相径向位移、液相径向位移和固相径向应力满足

$$\begin{cases}
 U_n^S(\bar{r}_n) = U_0^S(\bar{R}_0), \\
 U_n^F(\bar{r}_n) = U_0^F(\bar{R}_0), \\
 \bar{\sigma}_{nr}^{SE}(\bar{r}_n) = \sigma_0(\bar{R}_0).
 \end{cases} \quad (45)$$

综合考虑式(25)一式(30)、式(37)、式(38)、式

(40) 一式(45)可得

$$-A_{O1}h_0K_1(h_0\bar{R}_O)+\frac{1}{\bar{R}_O}D_{O1}=(a_{11}+a_{12})[A_{C1}K_1(q_C)+A_{C2}I_1(q_C)]-a_{13}[2K_1(q_C)+\frac{2-2\nu_C}{1-2\nu_C}q_CK_0(q_C)]\mu_C A_{C1}+a_{13}[\frac{2-2\nu_C}{1-2\nu_C}q_C I_0(q_C)-2I_1(q_C)]\mu_C A_{C2}, \quad (46)$$

$$\frac{h_0^2+\beta_{O1}}{\beta_{O2}}h_0K_1(h_0\bar{R}_O)A_{O1}-\frac{\beta_{O1}}{\beta_{O2}\bar{R}_O}D_{O1}=(a_{21}+a_{22})[A_{C1}K_1(q_C)+A_{C2}I_1(q_C)]-a_{23}[2K_1(q_C)+\frac{2-2\nu_C}{1-2\nu_C}q_CK_0(q_C)]\mu_C A_{C1}+a_{23}[\frac{2-2\nu_C}{1-2\nu_C}q_C I_0(q_C)-2I_1(q_C)]\mu_C A_{C2}, \quad (47)$$

$$[\frac{2-2\nu_O}{1-2\nu_O}h_0^2K_0(h_0\bar{R}_O)+h_0\frac{2}{\bar{R}_O}K_1(h_0\bar{R}_O)]A_{O1}-\frac{2}{\bar{R}_O}D_{O1}=(a_{31}+a_{32})[A_{C1}K_1(q_L)+A_{C2}I_1(q_C)]-a_{33}[2K_1(q_C)+\frac{2-2\nu_C}{1-2\nu_C}q_CK_0(q_C)]\mu_C A_{C1}+a_{33}[\frac{2-2\nu_C}{1-2\nu_C}q_C I_0(q_C)-2I_1(q_C)]\mu_C A_{C2}, \quad (48)$$

$$-[\frac{2}{\eta_0}K_1(q_C\eta_0)+\frac{2-2\nu_C}{1-2\nu_C}q_CK_0(q_C\eta_0)]\mu_C A_{C1}+[\frac{2-2\nu_C}{1-2\nu_C}q_C I_0(q_C\eta_0)-\frac{2}{r}I_1(q_C\eta_0)]\mu_C A_{C2}=Q, \quad (49)$$

由式(46)和式(47)可得

$$h_0^3K_1(h_0\bar{R}_O)A_{O1}=[\beta_{O1}(a_{11}+a_{12})+\beta_{O2}(a_{21}+a_{22})]\cdot[A_{C1}K_1(q_C)+A_{C2}I_1(q_C)]-(\beta_{O1}a_{13}+\beta_{O2}a_{23})\cdot[2K_1(q_C)+\frac{2-2\nu_C}{1-2\nu_C}q_CK_0(q_C)]\mu_C A_{C1}+(\beta_{O1}a_{13}+\beta_{O2}a_{23})\cdot[\frac{2-2\nu_C}{1-2\nu_C}q_C I_0(q_C)-2I_1(q_C)]\mu_C A_{C2}. \quad (50)$$

由式(46)和式(48)可得

$$h_0^3K_1(h_0\bar{R}_O)A_{O1}=[\beta_{O1}(a_{11}+a_{12})+\beta_{O2}(a_{21}+a_{22})]\cdot[A_{C1}K_1(q_C)+A_{C2}I_1(q_C)]-(\beta_{O1}a_{13}+\beta_{O2}a_{23})\cdot$$

$$[2K_1(q_C)+\frac{2-2\nu_C}{1-2\nu_C}q_CK_0(q_C)]\mu_C A_{C1}+(\beta_{O1}a_{13}+\beta_{O2}a_{23})\cdot[\frac{2-2\nu_C}{1-2\nu_C}q_C I_0(q_C)-2I_1(q_C)]\mu_C A_{C2}. \quad (51)$$

求解式(49)一式(51)可得

$$A_{C1}=\frac{(1-2\nu_C)\eta_0(b_{22}b_1-b_{12}b_2)}{(b_{22}b_1-b_{12}b_2)c_{11}+(b_{11}b_2-b_{21}b_1)c_{12}\mu_C}Q, \quad (52)$$

$$A_{C2}=\frac{(1-2\nu_C)\eta_0(b_{11}b_2-b_{21}b_1)}{(b_{22}b_1-b_{12}b_2)c_{11}+(b_{11}b_2-b_{21}b_1)c_{12}\mu_C}Q, \quad (53)$$

式中:

$$b_1=h_0^3K_1(h_0\bar{R}_O),$$

$$b_2=\frac{2-2\nu_O}{1-2\nu_O}h_0^2\bar{R}_OK_0(h_0\bar{R}_O),$$

$$b_{11}=[\beta_{O1}(a_{11}+a_{12})+\beta_{O2}(a_{21}+a_{22})]K_1(q_L)-(\beta_{O1}a_{13}+\beta_{O2}a_{23})[2K_1(q_L)+\frac{2-2\nu_L}{1-2\nu_L}q_LK_0(q_L)]\mu_L,$$

$$b_{12}=[\beta_{O1}(a_{11}+a_{12})+\beta_{O2}(a_{21}+a_{22})]I_1(q_L)+(\beta_{O1}a_{13}+\beta_{O2}a_{23})[\frac{2-2\nu_L}{1-2\nu_L}q_L I_0(q_L)-2I_1(q_L)]\mu_L,$$

$$b_{21}=[(a_{31}+a_{32})\bar{R}_O+2(a_{11}+a_{12})]K_1(q_L)-(\bar{R}_Oa_{33}+2a_{13})[2K_1(q_L)+\frac{2-2\nu_L}{1-2\nu_L}q_LK_0(q_L)]\mu_L,$$

$$b_{22}=[(a_{31}+a_{32})\bar{R}_O+2(a_{11}+a_{12})]I_1(q_L)+(\bar{R}_Oa_{33}+2a_{13})[\frac{2-2\nu_L}{1-2\nu_L}q_L I_0(q_L)-2I_1(q_L)]\mu_L,$$

$$c_{11}=-2(1-2\nu_L)\mu_LK_1(q_L\eta_0)-(2-2\nu_L)q_L\eta_0\mu_LK_0(q_L\eta_0),$$

$$c_{12}=(2-2\nu_L)q_L\eta_0\mu_L I_0(q_L\eta_0)-2(1-2\nu_L)\mu_L I_1(q_L\eta_0).$$

由此可以得到非均质饱和土与圆形隧道衬砌接触面处,饱和土固相的径向位移和径向应力分别为:

$$u=\frac{U_C(1)}{Q}=\frac{(1-2\nu_C)\eta_0[bb_1K_1(q_C)+bb_2I_1(q_C)]}{\mu_C(bb_1c_{11}+bb_2c_{12})}, \quad (54)$$

$$\phi=\frac{\bar{\sigma}_{Cr}(1)}{Q}=-\frac{2(1-2\nu_L)\eta_0bb_1K_1(q_L)}{bb_1c_{11}+bb_2c_{12}}-\frac{(2-2\nu_L)\eta_0bb_1q_LK_0(q_L)}{bb_1c_{11}+bb_2c_{12}}+$$

$$\frac{\eta_0 b b_2 [(2-2\nu_L)q_L I_0(q_L) - 2(1-2\nu_L)I_1(q_L)]}{b b_1 c_{11} + b b_2 c_{12}}, \quad (55)$$

式中: $b b_1 = b_{22} b_1 - b_{12} b_2$, $b b_2 = b_{11} b_2 - b_{21} b_1$ 。

4 数值算例与讨论

对于非均质特性和液相对径向非均质饱和土-圆形隧道衬砌稳态响应的影响,通过数值算例进行分析讨论。这里将非均质饱和土扰动区域划分为10个圈层,未做说明时各参数取值如下: $n_0^S = 0.67$, $n_0^F = 0.33$, $n_1^S = n_2^S = \dots = n_{10}^S = 0.67$, $n_1^F = n_2^F = \dots = n_{10}^F = 0.33$, $\nu_1 = \nu_2 = \dots = \nu_{10} = 0.33$, $\delta = 0.05$, $s_1 = s_2 = \dots = s_{10} = 0.33$, $m = 2.0$, $\rho_1 = \rho_2 = \dots = \rho_{10} = 1.0$, $s_0 = 0.01$, $\rho_{01} = \rho_{02} = \dots = \rho_{010} = 1/2$, $\nu_0 = 0.33$, $\nu_c = 0.33$, $\mu = 0.1$, $\mu_c = 2.0$, $\bar{R}_0 = 21$, $\bar{\rho}_c = 2.5$ 。

隧道周围土体与衬砌交界处饱和土固相径向位移和径向应力随频率变化曲线如图3和图4所示。

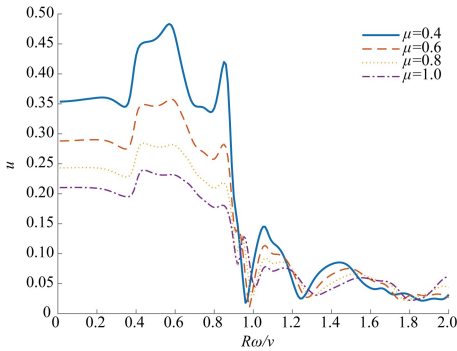


图3 影响区域剪切模量比不同时固相径向位移随频率变化曲线

Fig. 3 Curves of radial displacement of solid phase varying with frequency for different shear modulus ratio of influence region

可以看出,曲线存在较明显的波峰和波谷,径向非均质饱和土-圆形隧道衬砌系统存在共振现象。在无量纲频率 $R\omega/v = 1.0$ 附近,固相径向位移随频率变化存在较明显的下降,而径向应力随频率变化曲线则存在较明显的上升。从影响区域剪切模比 μ 对径向位移和径向应力的影响可以看出,扰动区域饱和土固相剪切模量的变化对非均质饱和土-圆形隧道衬砌系统动力响应的影响较大,且随着影响区域剪切模量比的增大,由于扰动造成隧道周围饱和土的弱化越小,饱和土强度增强,固相径向位移越小,而径向应力越大。因为影响区域剪切模量比对非均质饱和土-圆形隧道衬砌的影响较大,所以饱和土的非均质特性必须考虑。

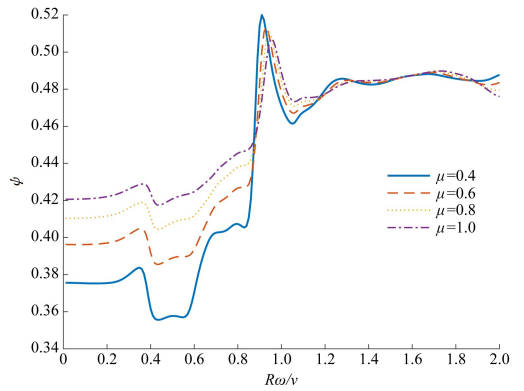


图4 影响区域剪切模量比不同时固相径向应力随频率变化曲线

Fig. 4 Curves of radial stress of solid phase varying with frequency for different shear modulus ratio of influence region

饱和土液固耦合系数对系统动力特性的影响见图5和图6,饱和土液固耦合系数对固相径向位移和径向应力的影响主要集中在峰值和谷值处,且液固耦合系数越大,径向位移和径向应力的峰值和谷值越大,且在耦合系数较大时,峰值和谷值增大较为明显,可见饱和土液固耦合系数对非均质饱和土-圆形隧道衬砌系统共振幅度的影响较大,需要引起关注。

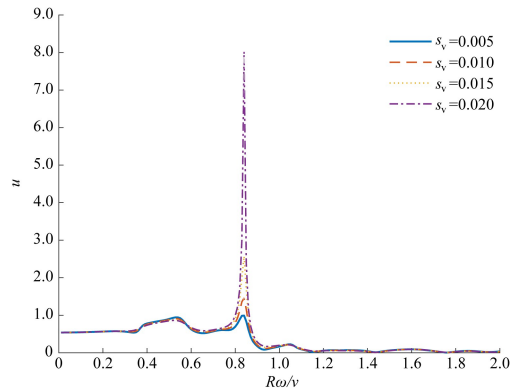


图5 液固耦合系数不同时固相径向位移随频率变化曲线

Fig. 5 Curves of radial displacement of solid phase varying with frequency for different liquid-solid coupling coefficient

非均质指数 m 对饱和土固相径向位移和径向应力的影响见图7和图8。可以看出,在低频时非均质指数 m 的影响非常大,非均质指数较小时 ($m=1$ 和 $m=2$ 时),饱和土固相径向位移和径向应力随频率变化曲线波动的较大,峰值较尖锐。非均质指数较大时 ($m=3$ 和 $m=4$ 时),饱和土固相径向位移和径向应力随频率变化曲线波动的较小,峰值较小。在高频时,非均质指数 m 对饱和土固相径向应力的影响较小。由于土体剪切模量沿径

向的变化对非均质饱和土-圆形隧道衬砌系统动力响应的影响较大,饱和土沿径向的非均质特性对系统动力特性的影响不能忽略,同时还需要选择准确的非均质指数刻画饱和土剪切模量沿径向的变化规律。

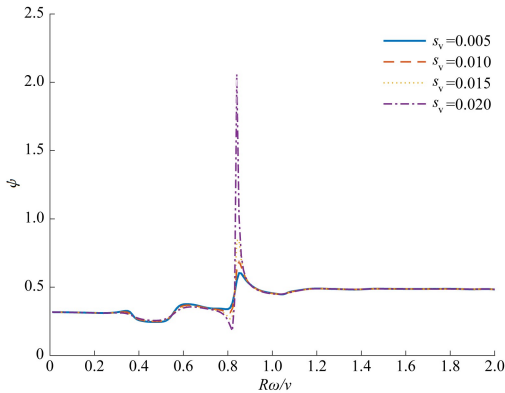


图6 液固耦合系数不同时
固相径向应力随频率变化曲线

Fig. 6 Curves of radial stress of solid phase varying with frequency for different liquid-solid coupling coefficient

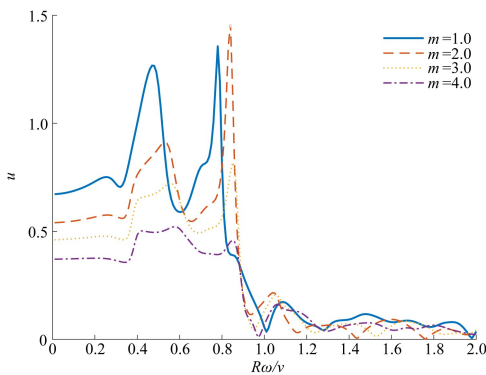


图7 非均质指数不同时
固相径向位移随频率变化曲线

Fig. 7 Curves of radial displacement of solid phase varying with frequency for different inhomogeneous index

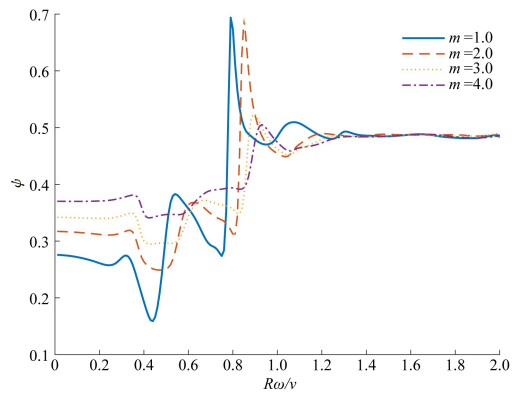


图8 非均质指数不同时
固相径向应力随频率变化曲线

Fig. 8 Curves of radial stress of solid phase varying with frequency for different inhomogeneous index

5 结论

为了考虑隧道周围土体非均质特性和土体液相对圆形隧道衬砌动力特性的影响,建立了径向非均质饱和土-圆形隧道衬砌模型,借助多图层传递法,得到了简谐内压力作用下径向非均质饱和土-圆形隧道衬砌稳态响应的解析解。通过数值算例,分析了饱和土和衬砌物理参量对非均质饱和土-圆形隧道衬砌动力特性的影响,得到的主要结论有:

(1)饱和土固相径向位移和径向应力随频率变化曲线在无量纲频率 $R\omega/v=1.0$ 附近存在较明显的突变。

(2)影响区域剪切模量比对非均质饱和土-圆形隧道衬砌的稳态响应有较大的影响,且土体剪切模量沿径向的变化规律对非均质饱和土-圆形隧道衬砌系统动力响应的影响也很大,圆形隧道周围饱和土的非均质特性必须考虑。

(3)饱和土液固耦合系数对固相骨架径向位移和径向应力随频率变化曲线的幅度的影响较大,主要集中的峰值和谷值处,液相对径向非均质饱和土-圆形隧道衬砌动力特性的影响,需要引起关注。

参考文献:

- [1] 王士革,高洪波,张宗领.基于损伤塑性理论的隧道衬砌结构开裂破坏的数值分析[J].信阳师范学院学报(自然科学版),2013,26(3):461-464.
WANG Shige, GAO Hongbo, ZHANG Zongling. Numerical analysis of cracking in lining structure of tunnel based on damage plasticity theory[J]. Journal of Xinyang Normal University (Natural Science Edition), 2013, 26(3): 461-464.
- [2] HUANG Jingqi, LI Huifang, CHEN Su, et al. Simplified analytical solutions for seismic response on cross section of circular tunnel with composite linings[J]. Computers and Geotechnics, 2021, 136: 104169.
- [3] 苏光北,狄宏规,周顺华,等.隧道施工期扰动对运营期隧道-土体系统动力响应的影响分析[J].振动与冲击,2023,42(15):210-218.
SU Guangbei, DI Honggui, ZHOU Shunhua, et al. Effects of disturbance during tunnel construction on dynamic

- response of tunnel-soil body system during tunnel construction period[J]. *Journal of Vibration and Shock*, 2023, 42(15): 210-218.
- [4] XIE Kanghe, LIU Ganbin, SHI Zuyuan. Dynamic response of partially sealed circular tunnel in viscoelastic saturated soil[J]. *Soil Dynamics and Earthquake Engineering*, 2004, 24(12): 1003-1011.
- [5] WANG Y, GAO G Y, YANG J. Three-dimensional dynamic response of a lined tunnel in a half-space of saturated soil under internal explosive loading[J]. *Soil Dynamics and Earthquake Engineering*, 2017, 101: 157-161.
- [6] HU Anfeng, LI Yijun, DENG Yuebao, et al. Vibration of layered saturated ground with a tunnel subjected to an underground moving load[J]. *Computers and Geotechnics*, 2020, 119: 103342.
- [7] EDELMAN I, WILMANSKI K. Asymptotic analysis of surface waves at vacuum/porous medium and liquid/porous medium interfaces[J]. *Continuum Mechanics and Thermodynamics*, 2002, 14(1): 25-44.
- [8] 高华喜, 闻敏杰, 张斌. 饱和黏弹性土中圆柱形隧洞的振动特性[J]. *振动工程学报*, 2012, 25(4): 380-387.
GAO Huaxi, WEN Minjie, ZHANG Bin. Vibration characteristics of a cylindrical tunnel in saturated viscoelastic soil[J]. *Journal of Vibration Engineering*, 2012, 25(4): 380-387.
- [9] 杨骁, 闻敏杰. 饱和和分数导数型黏弹性土-深埋圆形隧洞衬砌系统的动力特性[J]. *工程力学*, 2012, 29(12): 248-255.
YANG Xiao, WEN Minjie. Dynamic characteristics of saturated fractional derivative type viscoelastic soil and lining system with a deeply embedded circular tunnel[J]. *Engineering Mechanics*, 2012, 29(12): 248-255.
- [10] HAN Y C, SABIN G C W. Impedances for radially inhomogeneous viscoelastic soil media[J]. *Journal of Engineering Mechanics*, 1995, 121(9): 939-947.
- [11] NAGGAR E I, HESHAM M. Vertical and torsional soil reactions for radially inhomogeneous soil layer[J]. *Structural Engineering and Mechanics*, 2000, 10(4): 299-312.
- [12] DE BOER R, LIU Zhanfang. Propagation of acceleration waves in incompressible saturated porous solids[J]. *Transport in Porous Media*, 1995, 21(2): 163-173.
- [13] DE BOER R, LIU Zhanfang. Plane waves in a semi-infinite fluid saturated porous medium[J]. *Transport in Porous Media*, 1994, 16(2): 147-173.

责任编辑:郭红建

(上接第 497 页)

- [11] 宋少民, 周浩. 高吸附性机制砂石粉对防水砂浆性能的影响研究[J]. *新型建筑材料*, 2020, 47(1): 112-116.
SONG Shaomin, ZHOU Hao. Study on the effect of high adsorption stone powder on the performance of waterproof mortar[J]. *New Building Materials*, 2020, 47(1): 112-116.
- [12] 杨林, 刘亚明, 张冰, 等. 磷渣砂防水抗裂砂浆的性能及显微结构分析[J]. *混凝土*, 2015(2): 107-109.
YANG Lin, LIU Yaming, ZHANG Bing, et al. Analysis of performance and microstructure of waterproof and anti-crack phosphorus slag mortar[J]. *Concrete*, 2015(2): 107-109.
- [13] 张国防, 王培铭. E/VC/VL 三元共聚物对水泥砂浆孔结构和性能的影响[J]. *建筑材料学报*, 2013, 16(1): 111-114, 120.
ZHANG Guofang, WANG Peiming. Effects of ethylene/vinyl chloride/vinyl laurate redispersible terpolymer on pore structure and properties of cement mortar[J]. *Journal of Building Materials*, 2013, 16(1): 111-114, 120.
- [14] 靳昊, 易忠来, 温浩, 等. 内掺型有机硅防水剂对砂浆性能的影响[J]. *铁道建筑*, 2016(1): 89-91, 95.
JIN Hao, YI Zhonglai, WEN Hao, et al. Influence of internal mixing type organo-silicone waterproofing agent on mortar performance[J]. *Railway Engineering*, 2016(1): 89-91, 95.
- [15] 中华人民共和国住房和城乡建设部. 建筑砂浆基本性能试验方法标准: JGJ/T 70—2009[S]. 北京: 中国建筑工业出版社, 2009.
Ministry of Housing and Urban Rural Development of the People's Republic of China. Standard for test method of basic properties of construction mortar: JGJ/T 70—2009[S]. Beijing: China Architecture & Building Press, 2009.
- [16] 国家市场监督管理总局, 国家标准化管理委员会. 水泥胶砂强度检验方法(ISO 法): GB/T 17671—2021[S]. 北京: 中国标准出版社, 2021.
State Administration for Market Regulation, Standardization Administration of China. Test method of cement mortar strength(ISO method): GB/T 17671—2021[S]. Beijing: Standards Press of China, 2021.
- [17] 中华人民共和国国家发展和改革委员会. 聚合物改性水泥砂浆试验规程: DL/T 5126—2001[S]. 北京: 中国电力出版社, 2001.
National Development and Reform Commission of the People's Republic of China. Test code on polymer-modified cement mortar: DL/T 5126—2001[S]. Beijing: China Electric Power Press, 2001.

责任编辑:郭红建